

INFORMATION TO USERS

This manuscript has been reproduced from the microfilm master. UMI films the text directly from the original or copy submitted. Thus, some thesis and dissertation copies are in typewriter face, while others may be from any type of computer printer.

The quality of this reproduction is dependent upon the quality of the copy submitted. Broken or indistinct print, colored or poor quality illustrations and photographs, print bleedthrough, substandard margins, and improper alignment can adversely affect reproduction.

In the unlikely event that the author did not send UMI a complete manuscript and there are missing pages, these will be noted. Also, if unauthorized copyright material had to be removed, a note will indicate the deletion.

Oversize materials (e.g., maps, drawings, charts) are reproduced by sectioning the original, beginning at the upper left-hand corner and continuing from left to right in equal sections with small overlaps.

Photographs included in the original manuscript have been reproduced xerographically in this copy. Higher quality 6" x 9" black and white photographic prints are available for any photographs or illustrations appearing in this copy for an additional charge. Contact UMI directly to order.

Bell & Howell Information and Learning
300 North Zeeb Road, Ann Arbor, MI 48106-1346 USA
800-521-0600

UMI[®]

PREVIEW

CONTAMINANT TRANSPORT IN HIGH-CAPACITY PUMPING SETTING WITH
A VERTICAL GROUNDWATER FLOW COMPONENT:
FIELD TRACER EXPERIMENTS AND NUMERICAL MODELING

by

Vikas Tandon

A DISSERTATION

Presented to the Faculty of

The Graduate College at the University of Nebraska

In Partial Fulfillment of Requirements

For the Degree of Doctor of Philosophy

Major: Geosciences (Hydrogeology)

Under the Supervision of Professor Vitaly A. Zlotnik

Lincoln, Nebraska

December, 2000

UMI Number: 9997020

PREVIEW

UMI[®]

UMI Microform 9997020

Copyright 2001 by Bell & Howell Information and Learning Company.

All rights reserved. This microform edition is protected against
unauthorized copying under Title 17, United States Code.

Bell & Howell Information and Learning Company
300 North Zeeb Road
P.O. Box 1346
Ann Arbor, MI 48106-1346

DISSERTATION TITLE

Contaminant Transport In High-Capacity Pumping Setting With A Vertical

Groundwater Flow Component: Field Tracer Experiments And Numerical Modeling

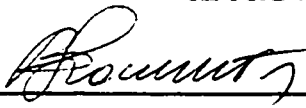
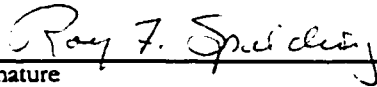
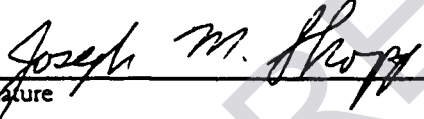

BY

Vikas Tandon

SUPERVISORY COMMITTEE:

APPROVED

DATE

<u></u>	<u>12-05-00</u>
Signature	
<u>Dr. Vitaly A. Zlotnik</u>	
Typed Name	
<u></u>	<u>12-05-00</u>
Signature	
<u>Dr. Roy F. Spalding</u>	
Typed Name	
<u></u>	<u>Dec. 5, 2000</u>
Signature	
<u>Dr. Joseph M. Skopp</u>	
Typed Name	
<u></u>	<u>12/5/2000</u>
Signature	
<u>Dr. Wayne Woldt</u>	
Typed Name	
<u></u>	
Signature	
<u></u>	
Typed Name	
<u></u>	
Signature	
<u></u>	
Typed Name	

CONTAMINANT TRANSPORT IN HIGH-CAPACITY PUMPING SETTING WITH A
VERTICAL GROUNDWATER FLOW COMPONENT:
FIELD TRACER EXPERIMENTS AND NUMERICAL MODELING

Vikas Tandon, Ph.D.

University of Nebraska, 2000

Advisor: Vitaly A. Zlotnik

This study investigates the extent and impact of vertical flow on solute transport in groundwater at the Nebraska MSEA site. Three tracer tests, designed with a geometrical configuration suitable for the detection of vertical flow, were conducted. As the tracer plume moved towards the extraction wells, it bifurcated into two plumes, with the deeper plume travelling at a velocity two to four times higher than the shallow plume. The deeper plume exhibited a vertical displacement of 4 m over a horizontal distance of 13 m.

Multilevel slug tests, grain size analyses, and pumping tests were performed to produce a three-dimensional hydraulic conductivity data base. Preferential pathways for contaminant movement were identified. A low conductivity zone was observed above the 7.3 m depth; while a high conductivity zone was observed towards the aquifer base. The inverse distance weighted technique was used to interpolate hydraulic conductivity values at locations for which measured values were not available.

Three-dimensional flow and transport modeling was used to simulate tracer test 3. The model predictions were found to be strongly sensitive to the variability of hydraulic conductivity and the anisotropy ratio, moderately sensitive to porosity, and least sensitive to dispersivity. The quality of simulations was similar to those reported by Yeh et al. (1995). Peak arrival time was better replicated by the MSEA model, while Yeh et al. model replicated peak relative concentration more accurately. Simulation results were also compared with observed data using temporal moments. The model predicted average travel time more accurately as compared to the absolute integral area.

The MSEA model was able to replicate the bulk movement of the plume with higher degree of certainty than the predictions at individual measurement points. The magnitude of vertical mixing observed implies that the prediction of contaminant transport in agricultural settings must incorporate two key factors: a) vertical displacement of contaminant trajectories due to pumping for irrigation, and b) preferential pathways created by aquifer heterogeneity.

Acknowledgements

I would like to thank the individuals and institutions that enabled me to conduct the research culminating in this doctoral dissertation. Special thanks are due to my graduate advisor, Dr. Vitaly Zlotnik, for his untiring guidance and support of the research effort. Thanks are also extended to members of my research committee: Dr. Roy Spalding, Dr. Wayne Woldt, and Dr. Joseph Skopp. I would like to thank the Department of Geosciences and the Water Sciences Laboratory at the University of Nebraska-Lincoln; the Hydrogeology Division of the Geological Survey of America; Central Platte Natural Resources District, Grand Island, Nebraska; and Nebraska Geological Society for their support to the research project. I would like this opportunity to thank fellow graduate students Brian Zurbuchen, Mark Ferlin, Virginia McGuire, and Ron Ramold for their help during different phases of the research.

In addition, I would like to thank my wife, Polly, for her support, patience and understanding through the completion of the degree program. Special thanks are due to my baby daughter Suneeta, for the her buoyant smiles during the last phases of writing.

TABLE OF CONTENTS

ABSTRACT

ACKNOWLEDGMENTS

LIST OF FIGURES

LIST OF TABLES

LIST OF APPENDICES

1.0	INTRODUCTION.....	1
1.1	Investigation Background and Overview.....	1
1.2	Specific Goals and Objectives of the Investigation.....	3
1.3	Investigation Approach.....	4
1.4	Literature Review.....	8
2.0	SITE GEOLOGY AND HYDROGEOLOGY.....	12
2.1	Site Location and Description.....	12
2.2	Site Geology.....	12
2.2.1	Borehole sampling.....	13
2.2.2	Lithologic profiles.....	13
2.3	Site Hydrogeology	15
2.3.1	Water level monitoring	15

2.3.2	Groundwater flow delineation.....	18
3.0	CHARACTERIZATION OF AQUIFER HYDRAULIC CONDUCTIVITY.....	21
3.1	Methods Employed for Hydraulic Conductivity Determination.....	21
3.2	Well Design and Locations.....	22
3.3	Pumping Tests.....	23
3.3.1	Test configuration and description.....	23
3.3.2	Test analysis techniques and interpretation.....	28
3.3.3	Test results.....	31
3.4	Multilevel Slug Tests.....	32
3.4.1	Test configuration and description.....	32
3.4.2	Test results.....	33
3.5	Grain-Size Analysis.....	34
3.5.1	Techniques employed.....	34
3.5.2	Results and interpretation.....	35
3.6	Interpolation of Aquifer Hydraulic Conductivities.....	35
3.6.1	Spatial discretization requirements.....	39
3.6.2	Tools available and their applicability.....	41
3.6.3	Interpolation approaches.....	44
3.6.3.1	Inverse distance weighing : layered approach.....	44
3.6.3.2	Inverse distance weighing : 3-dimensional approach.....	46

3.6.3.3	Comparison with grain-size based distributions.....	56
3.7	Overall Assessment of Site Hydrostratigraphic Architecture.....	57
4.0	DESIGN OF TRACER TESTS WITH VERTICAL FLOW COMPONENT.....	59
4.1	Objectives of Test Design.....	59
4.2	Factors Controlling Vertical Movement.....	60
4.2.1	Injection-extraction well separation.....	60
4.2.2	Depth of injection and extraction centers.....	62
4.2.3	Tracer injection and plume inception.....	63
4.2.4	Extraction rates.....	63
4.2.5	Disposition of extracted water.....	65
4.2.6	Temperature convection effects.....	66
4.3	3-D Geometrical Design and Instrumentation of Tests.....	67
4.3.1	Hydraulic design.....	67
4.3.2	Instrumentation.....	67
5.0	NATURAL GRADIENT TRACER TEST.....	71
5.1	Hydraulic Regime Monitoring.....	71
5.2	Test Schematics.....	72
5.2.1	Tracer injection.....	72
5.2.2	Plume monitoring.....	72

5.3	Results and interpretation.....	74
6.0	FORCED GRADIENT TRACER TEST 1.....	75
6.1	Hydraulic Regime Monitoring.....	75
6.2	Test Schematics.....	77
6.2.1	Tracer injection.....	77
6.2.2	Plume monitoring.....	78
6.3	Breakthrough Curve Analysis.....	78
6.4	Spatial Concentration Fields.....	84
6.5	Trends in Plume Movement.....	90
7.0	FORCED GRADIENT TRACER TEST 2.....	94
7.1	Hydraulic Regime Monitoring.....	94
7.2	Test Schematics.....	96
7.2.1	Tracer injection.....	96
7.2.2	Plume monitoring.....	96
7.3	Breakthrough Curve Analysis.....	97
7.4	Trends in Plume Movement.....	104
8.0	FORCED GRADIENT TRACER TEST 3.....	111
8.1	Hydraulic Regime Monitoring.....	111

8.2	Test Schematics.....	113
8.2.1	Tracer injection.....	113
8.2.2	Plume monitoring.....	113
8.3	Breakthrough Curve Analysis.....	114
8.4	Trends in Plume Movement.....	118
9.0	NUMERICAL MODELING OF VERTICAL CONTAMINANT TRANSPORT.....	126
9.1	Modeling Objectives.....	126
9.2	Modeling Approach.....	127
9.3	Flow Model.....	129
9.3.1	Model construction.....	130
9.3.1.1	Spatial discretization.....	131
9.3.1.2	Temporal discretization.....	131
9.3.2	Input parameters.....	134
9.3.3	Model calibration.....	134
9.3.3.1	Hydraulic conductivity	137
9.3.3.2	Anisotropy.....	139
9.3.3.3	Storage.....	141
9.3.3.4	Specific yield.....	143
9.3.4	Results.....	145

9.4	Transport Model.....	150
9.4.1	Model construction.....	151
9.4.2	Input parameters.....	151
9.4.3	Model calibration.....	152
9.4.3.1	Porosity.....	153
9.4.3.2	Dispersivity.....	159
9.4.4	Results.....	163
10.0	DISCUSSION.....	179
10.1	Conceptual Overview of Agri-Chemical Movement in Groundwater....	179
10.2	Field Testing Based Evidence of Vertical Transport Component.....	180
10.3	Heterogeneity Characterization.....	200
10.4	Model Predictions and Summary of Results.....	202
11.0	CONCLUSIONS.....	219
REFERENCES		

LIST OF TABLES

Table 1	Location and construction details of the observation well network for the MSEA pumping tests
Table 2	Aquifer Parameters obtained from pumping tests at the MSEA site
Table 3	Hydraulic conductivity estimates from multilevel slug tests at the MSEA site
Table 4	Resolution of hydraulic conductivity measurements versus model requirements at select sites
Table 5	Statistical comparison of grain size based and inverse distance weight interpolated $\ln(K)$ distribution
Table 6	Model spatial discretization parameters
Table 7 a	Flow simulation calibration target summary
Table 7 b	Flow simulation variable modification summary

Table 8	Flow model calibration -horizontal hydraulic conductivity data set
Table 9	Flow model calibration - anisotropy ratios
Table 10	Flow model calibration - storage coefficients
Table 11	Flow model calibration - specific yield
Table 12	Calibrated flow model: Error analysis
Table 13	Transport model design parameters
Table 14 a	Transport model calibration - advective flow, porosity =0.30
Table 14 b	Transport model calibration - advective flow, porosity =0.20
Table 14 c	Transport model calibration - advective flow, porosity =0.25
Table 14 d	Transport model calibration - advective flow, porosity =0.35

Table 15 a	Transport model calibration - porosity =0.30, α_L =0.20 m
Table 15 b	Transport model calibration - porosity =0.30, α_L =0.50 m
Table 15 c	Transport model calibration - porosity =0.30, α_L =1.00 m
Table 16	Breakthrough curve quality analysis - Yeh et al. data set (May 1992 test)
Table 17	Breakthrough curve quality analysis - Tracer test 3 simulation
Table 18	Breakthrough curve match classification based on error in estimating peak arrival time
Table 19	Breakthrough curve match classification based on error in estimating peak relative concentration
Table 20	Forced gradient tracer test 3: Comparison of observed and simulated absolute integral areas under breakthrough curves, average travel times and peak concentrations

LIST OF FIGURES

- Fig. 1 Site Location
- Fig. 2 Geologic cross-section across the MSEA site
- Fig. 3 Representative cross-section of the unconfined aquifer beneath the MSEA site
- Fig. 4 Location map depicting MLS array used for groundwater mapping
- Fig. 5 Potentiometric map for the unconfined aquifer beneath the MSEA
- Fig. 6 Cluster 1 wells at the MSEA site
- Fig. 7 Cluster 2 wells at the MSEA site
- Fig. 8 Cluster 3 wells at the MSEA site
- Fig. 9 Unconfined aquifer type curves for time versus drawdown showing the effect of delayed yield

- Fig. 10 Hydraulic conductivity profiles for wells along the injection-extraction axis
- Fig. 11 Hydraulic conductivity profiles for wells across the injection-extraction axis
- Fig. 12 Stratified hydraulic conductivity distribution: plan view of layer 5
- Fig. 13 Stratified hydraulic conductivity distribution: cross sectional view along the injection extraction axis
- Fig. 14 3-dimensional hydraulic conductivity field: plan view of layer 5
- Fig. 15 3-dimensional hydraulic conductivity field: cross sectional view along the injection extraction axis
- Fig. 16 Discrepancy in the estimation of mean $\ln(k)$ obtained by using the IDWN approaches
- Fig. 17 Discrepancy in the estimation of $\ln(k)$ variances obtained by using the IDWN approaches

- Fig. 18 a Plan view of tracer test well field (english units)
- Fig. 18 b Plan view of tracer test well field (metric units)
- Fig. 19 Aquifer cross section and well layout along the axis of tracer movement
- Fig. 20 Natural Gradient Tracer Test: Breakthrough curves at well IW1
- Fig. 21 Forced gradient tracer test 1: Extraction schedule
- Fig. 22 a Forced gradient tracer test 1: Breakthrough curves at IW2
- Fig. 22 b Forced gradient tracer test 1: Breakthrough curves at A2, shallow levels
- Fig. 22 c Forced gradient tracer test 1: Breakthrough curves at A2, middle levels
- Fig. 22 d Forced gradient tracer test 1: Breakthrough curves at A2, deeper levels
- Fig. 22 e Forced gradient tracer test 1: Breakthrough curves at ML14, shallow levels
- Fig. 22 f Forced gradient tracer test 1: Breakthrough curves at ML14, deeper levels

- Fig. 22 g Forced gradient tracer test 1: Breakthrough curves at B1, middle levels
- Fig. 22 h Forced gradient tracer test 1: Breakthrough curves at B1, deeper levels
- Fig. 23 a Forced gradient tracer test 1: Normalized concentration distribution 2.2 days after injection
- Fig. 23 b Forced gradient tracer test 1: Normalized concentration distribution 4.0 days after injection
- Fig. 23 c Forced gradient tracer test 1: Normalized concentration distribution 7.5 days after injection
- Fig. 23 d Forced gradient tracer test 1: Normalized concentration distribution 16.0 days after injection
- Fig. 23 e Forced gradient tracer test 1: Normalized concentration distribution 27 days after injection
- Fig. 24 Forced gradient tracer test 2: Extraction schedule

- Fig. 25 a Forced gradient tracer test 2: Breakthrough curves at IW2
- Fig. 25 b Forced gradient tracer test 2: Breakthrough curves at A2, shallow levels
- Fig. 25 c Forced gradient tracer test 2: Breakthrough curves at A2, middle levels
- Fig. 25 d Forced gradient tracer test 2: Breakthrough curves at A2, deeper levels
- Fig. 25 e Forced gradient tracer test 2: Breakthrough curves at ML14, shallow
levels
- Fig. 25 f Forced gradient tracer test 2: Breakthrough curves at ML14, deeper levels
- Fig. 25 g Forced gradient tracer test 2: Breakthrough curves at B1, shallow levels
- Fig. 25 h Forced gradient tracer test 2: Breakthrough curves at B1, middle levels
- Fig. 25 i Forced gradient tracer test 2: Breakthrough curves at B1, deeper levels
- Fig. 25 j Forced gradient tracer test 2: Normalized concentration distribution 1 day
after injection

- Fig. 25 k Forced gradient tracer test 2: Normalized concentration distribution 2 days after injection
- Fig. 25 l Forced gradient tracer test 2: Normalized concentration distribution 4 days after injection
- Fig. 25 m Forced gradient tracer test 2: Normalized concentration distribution 6 days after injection
- Fig. 26 Forced gradient tracer test 3: Extraction schedule
- Fig. 27 a Forced gradient tracer test 3: Breakthrough curves at $\Gamma W2$
- Fig. 27 b Forced gradient tracer test 3: Breakthrough curves at A2, middle levels
- Fig. 27 c Forced gradient tracer test 3: Breakthrough curves at A2, deeper levels
- Fig. 27 d Forced gradient tracer test 3: Breakthrough curves at ML14, middle levels
- Fig. 27 e Forced gradient tracer test 3: Breakthrough curves at B1, middle levels

- Fig. 27 f Forced gradient tracer test 3: Breakthrough curves at B1, deeper levels
- Fig. 27 g Forced gradient tracer test 3: Normalized concentration distribution 1 day after injection
- Fig. 27 h Forced gradient tracer test 3: Normalized concentration distribution 2 days after injection
- Fig. 27 i Forced gradient tracer test 3: Normalized concentration distribution 4 days after injection
- Fig. 27 j Forced gradient tracer test 3: Normalized concentration distribution 6 days after injection
- Fig. 28 Plan view of the three-dimensional finite difference grid used for modeling.
- Fig. 29 a Model vs observed drawdowns at IW1, IW2 and IW3
- Fig. 29 b Model vs observed drawdowns at A1 and A2